Damage sources for the NIF Grating Debris Shield (GDS) and methods for their mitigation

C. W. CARR*, J. BUDE, P. E. MILLER, T. PARHAM, P. WHITMAN, M. MONTICELLI, R. RAMAN, D. CROSS, B. WELDAY, F. RAVIZZA, T. SURATWALA, J. DAVIS, M. FISCHER, R. HAWLEY, H. LEE, M. MATTHEWS, M. NORTON, M. NOSTRAND, D. VANBLARCOM, AND S. SOMMER

Lawrence Livermore National Laboratory, 7000 East Avenue, Livermore, California, 94550, USA

ABSTRACT

The primary sources of damage on the National Ignition Facility (NIF) Grating Debris Shield (GDS) are attributed to two independent types of laser-induced particulates. The first comes from the eruptions of bulk damage in a disposable debris shield downstream of the GDS. The second particle source comes from stray light focusing on absorbing glass armor at higher than expected fluences. We show that the composition of the particles is secondary to the energetics of their delivery, such that particles from either source are essentially benign if they arrive at the GDS with low temperatures and velocities.

1. INTRODUCTION

High energy lasers, such as the National Ignition Facility[1] (NIF) and The Laser Megajoule[2] are ultimately limited in operation by laser-induced damage (LID) of their optical components[3]. On NIF the grating debris shield (GDS) has historically been the final NIF optic that is most prone to damage. Damage on the GDS typically manifests as individual sites a few tens of microns in diameter[4]. As initiated, this damage would be of little consequence to laser operation. Unfortunately, this type of damage grows rapidly upon subsequent illumination with laser light, necessitating removal and repair[5, 6] of the optic within a few months[7, 8].

This propensity of the GDS to damage more than other final optics can be seen by comparing the number of growing damage sites on all NIF GDS optics to the number on the wedged focus lenses (WFL) (figure 1). Furthermore, improvements to optics surface quality were only partially successful in improving the damage resistance to the GDS. Log growth is a single parameter metric derived from the growth predicted by the growth rule

$$d_n = d_0 e^{\alpha n} \quad (1)$$

for exit surface sites on SiO_2.

Where d is the site diameter, n is the shot number, and α is the growth rate. The log growth of a shot or sequence of shots

$$\text{Log Growth} = \ln(\langle d_n \rangle / d_0) \quad (2)$$

Laser-Induced Damage in Optical Materials 2017, edited by Gregory J. Exarhos, Vitaly E. Gruzdev, Joseph A. Menapace, Detlev Ristau, MJ Soileau, Proc. of SPIE Vol. 10447, 1044702
 · doi: 10.1117/12.2281202

is the natural log of expected final size of an exit surface site on SiO_2 divided by it's starting size as predicted by established fused silica growth rules[9-11]

Figure 1 shows the damage rates of the WFL and GDS before development of the advanced mitigation process[12, 13] (AMP) as well as the rates and projections after the implementation of AMP as a function of log growth (LG)[7, 9, 14]. The AMP2 (rev 2 of the AMP process) expected line for the WFL and GDS are derived from numerous off-line experiments which established the damage density as a function of fluence ($\rho(\phi)$) expected for SiO_2 surfaces treated with the AMP2 process and the incident fluence distribution for each optic type (see figure 2). The reduction in initiation rate of the GDS is both qualitatively less than observed on the WFL as well as inconsistent with the AMP2 $\rho(\phi)$. As the model accurately projects the initiation rate on the SiO_2 WFL, but not the GDS, we conclude that the difference in the GDS performance is due to environmental factors[15-17].

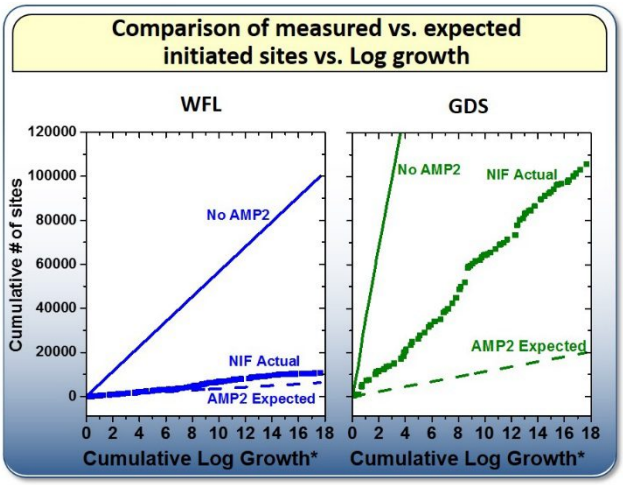

Figure 1. Damage initiation rate on SiO_2 WFLs and GDSs optics both before and after the implementation of the AMP2 process. Dashed lines show the expected initiation rates for both optic types based on $\rho(\phi)$ measurements

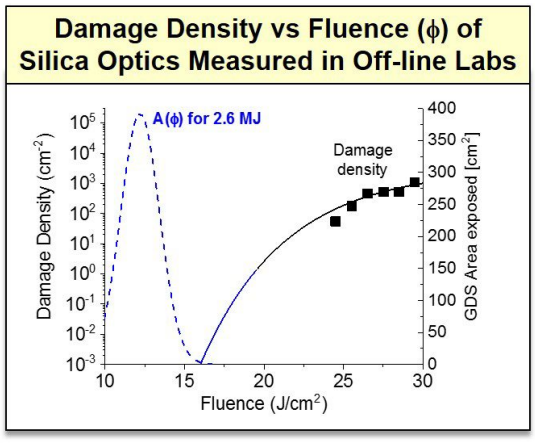

Figure2. Damage density as a function of fluence ($\rho(\phi)$) for AMP2 surfaces measured in off-line labs and the hypothetical fluence distribution seen by a GDS optic when utilized for a 2.6 MJ shot on NIF.

2. UNEXPECTED DAMAGE AND MITIGATIONS

The observed morphology of the damage from NIF optics used during operations was our first indicator of the source of the damage. Damage sites generated in off-line labs are typically monolithic while many of the smaller sites observed on NIF optics are accompanied by satellite features (see figure 3). Medium sized sites (50 – 150 microns in diameter) on NIF GDS optics are often monolithic but have shallower aspect ratios to classic sites. By the time sites on a GDS are ready for repair at 300 microns, they have generally resumed a monolithic morphology with a 3:1 width to depth aspect ratio[18]. We also find fields of features similar to those surrounding damage sites on the surface without damage associated with them.

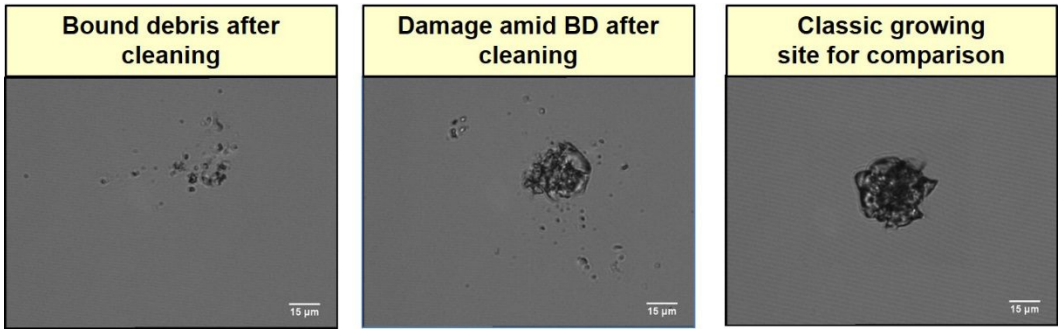

Figure 3. Left: field of debris found on the surface of GDS optics after removal from NIF. Center: A damage on the site surrounded by a debris field from the same GDS. Right: a damage site generated in an off-line lab

Inspection of the debris show that they are not removed by the standard NIF optics cleaning protocol which includes ultrasonic agitation in hot NaOH, but can be partially removed by drag wiping. Samples of particles found on the surface of the optic were tested with EDX spectroscopy and found to primarily consist of Borofloat® glass (see figure 4). Most particles appeared to have a melted or at least partially melted appearance.

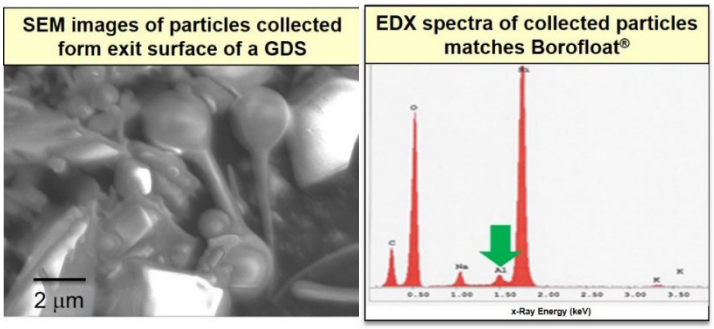

Figure 4. Left: SEM image of particles collected from the exit surface of a GDS from NIF. Right EDX spectra of the collected particles is a match for Borofloat®.

Figure 5 shows a schematic of the optical layout in the region of the GDS. The disposable debris shield (DDS) is immediately downstream of the GDS and the only optic in NIF composed of Borofloat®[19] glass.

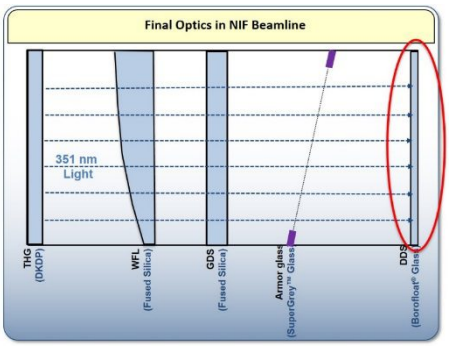

Figure 5. A schematic of the optical components surrounding the GDS in a NIF beam line.

Testing and examination of the DDS reveals no surface damage at fluences below 20 J/cm^2 with 3 ns 3ω pulses and then only on the exit surface (facing away from the GDS). This is well above the fluence DDS optics are exposed to on NIF. Bulk damage, however, is quite common. This damage, which occurs at fluences above about 6 J/cm^2 will quickly grow towards the input surface and erupt (see figure 6). The rate of growth toward the input surface (figure 7) and the amount of material ejected once erupted was measured offline (figure 13). The bulk damage is relatively sparse and localized, but is equally likely to occur in all locations through the bulk of the DDS. This suggests that the source of the bulk damage is inclusions incorporated during fabrication, and not related to surface contamination or flaws.

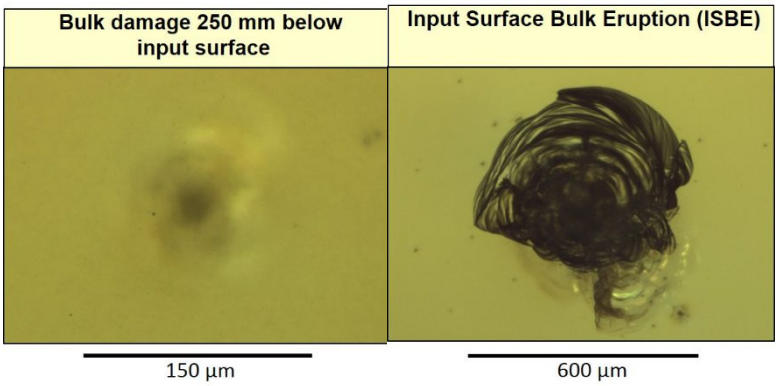

Figure 6. Left: A bulk damage site situated 250 microns below the input surface of a DDS. Right: A bulk damage site which has grown to the surface and erupted. Satellite bulk initiations surrounding the primary damage site are common and may be due to smaller inclusions or stress induced in the glass which lowers its damage threshold.

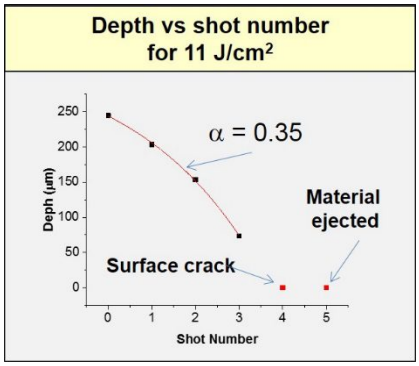

Figure 7. Depth vs shot number for the bulk damage site shown in figure 6 at 11 J/cm^2 . The bulk damage site initially damaged while its host DDS was installed on NIF and was grown in an off-line lab. The site breached the input surface on the 4th laboratory shot but did not emit significant ejecta until the fifth shot.

In order to test if the particles ejected from an ISBE are responsible for damage on the GDS we excised a number of 2-inch square sections of DDS centered on ISBEs. An ISBE was installed in a test chamber of the Optical Science Laser (Ref UCRL-CONF-155394) with a SiO_2 window placed 4 cm downstream (see figure 8). The two samples were exposed to various levels of 3ω fluence and the particles ejected from the ISBE collected on the second sample were cataloged with a robotic microscope and SEM. Before damage testing the collected particles, a portion were transferred to another sample. Although both samples have particles generated by the same ISBE on the same shot they differ in that the first sample had its particles deposited directly from the ISBE and the second sample had indirectly deposited particles. The directly deposited particles would have arrived at high velocity and at high temperature[16]. The indirectly deposited particles would have arrived near ambient temperature and with low velocities and have lower adhesion to the surface.

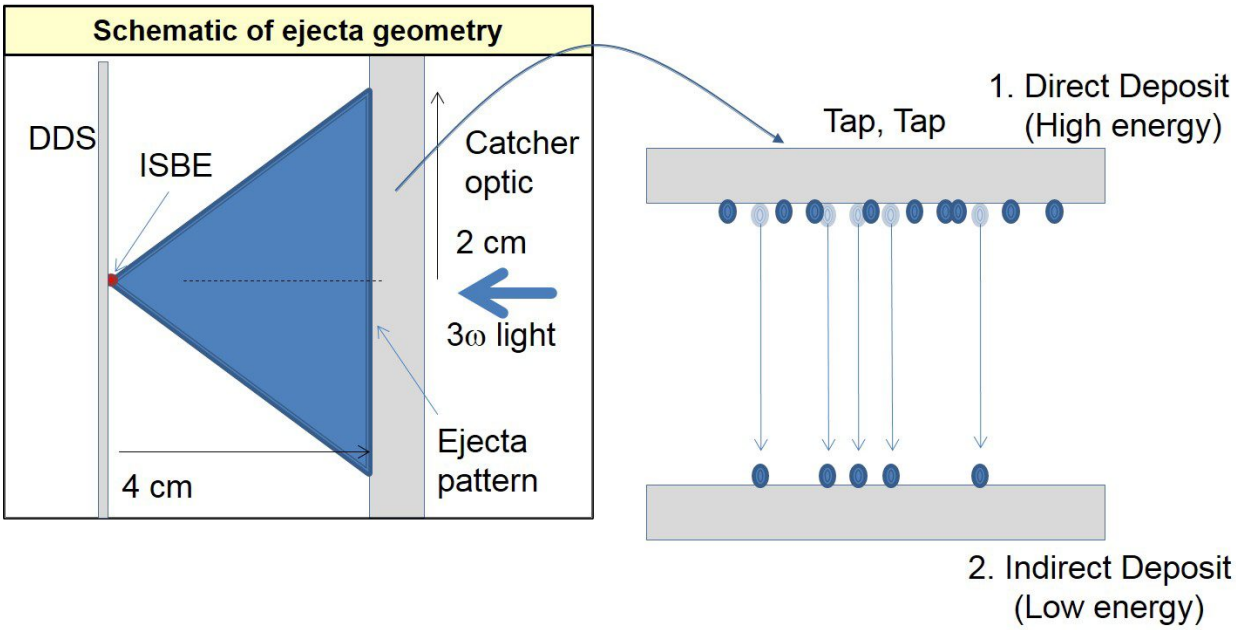

Figure 8. Left: Schematic of particle collection experiment in OSL. Right: Transfer of particles from collection optic to 2nd damage test sample.

The two samples were then sequentially tested in OSL with 9-J/cm^2 3ω 5-ns flat in time or FIT pulses. The laser exposure caused the majority of particles on both samples to either induce damage to the substrate or be removed without inducing damage (cleaned). Here damage is defined as inducing a fracture in the substrate, as without a fracture growth does not occur. The fraction of particles by size which damaged can be seen in figure 9. The probability that directly deposited particles would damage when exposed to the 9-J/cm^2 test pulse exceeded 0.5 for particles sizes over about 10 microns in diameter. The particles that were tested after cold transfer did not damage after a single 9-J/cm^2 shot. A number of the larger particles did splatter (without inducing visible fracture in the substrate) during the first test pulse and proceeded to damage after a second test pulse. This behavior is similar to that observed by Matthews et al. when samples were seeded with glass spheres[20].

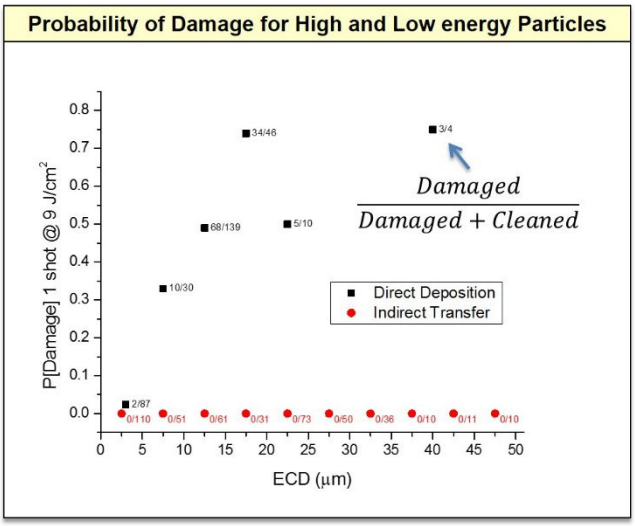

Figure 9. Probability of damage for both directly and indirectly deposited particles exposed to 9-J/cm^2 3ω 5-ns pulses. Almost all particles were removed without damaging the substrate (cleaned) or produced clear damage.

The morphology of the directly deposited particles are similar to the debris fields observed on NIF GDS optics. SEM pictures of the directly deposited particles before and after exposure to the 9 J/cm^2 laser pulse can be seen in figure 10. Evidence of substrate fracture can be seen in some of the images acquired before laser exposure, suggesting that the particles occasionally produce fractures in the substrate on impact. This phenomenon, intentionally over-represented here, is visible in about 5% of randomly selected SEM images of this resolution. We also note that all debris show evidence of being at least partial, if not entirely, melted. This raises the question whether the physical factor that makes directly deposited particles prone to initiating damage is due to greater adhesion of molten material or fracture induced on impact.

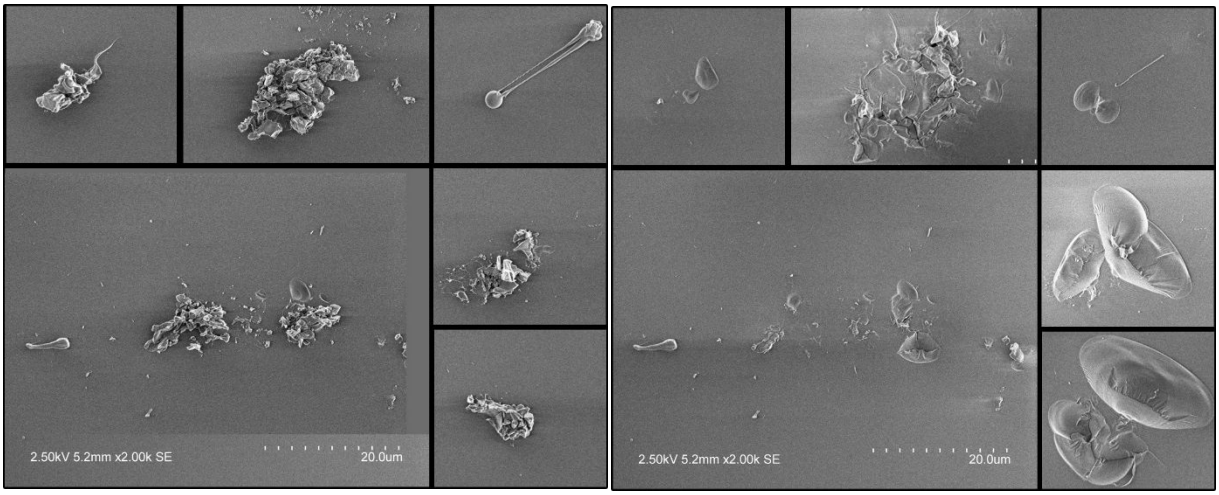

Figure 10. SEM images of directly deposited particles before (left) and after (right) of exposure to a 9 J/cm^2 pulse.

In order to both test the hypothesis that particles ejected from input surface bulk eruptions (ISBE) on the disposable debris shield were a primary source of damage as well as a potential mitigation, an experiment was conducted on NIF where an additional optic was placed in the beam line in between the GDS and the DDS. This optic was fabricated from SiO_2 and therefore did not have the same inclusions as the Borofloat® DDS which cause the ISBEs. The experiment, which is detailed elsewhere[21], consisted of inserting SiO_2 screens in four of eight test beams with the expectation that damage would be eliminated on the beams with the screens. What was found instead is spatially distinct patterns of damage that were not visible previously (see figure 11). The highly localized damage was not consistent with damage produced by ISBE ejecta which may be concentrated in a specific random location on an optic, but not in similar locations across several optics.

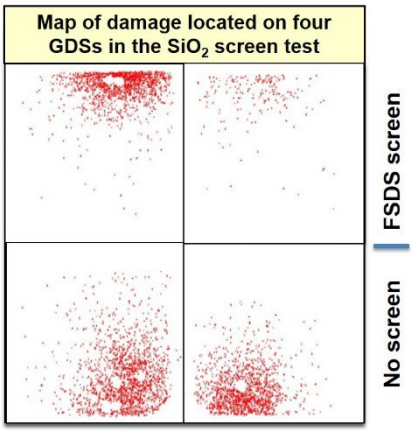

Figure 11. Map of damage on the four GDS optics in a NIF Quad. The two upper optics had SiO_2 screens in place while the two lower optics did not. Each red dot represents a damage site on the optic. Between the anomalous spatial patterning and new primary particle composition a second damage source seemed likely.

Particles collected from these regions exhibited an EDX spectra consistent with a composition of SuperGrey™[22] rather than Borofloat® glass. SuperGrey™ is used in NIF beam lines as armoring to absorb stray reflections before they encounter the beam tube walls. Review of the known ghosts in the region of the exits surface of the GDS found that the m = 2 reflection from the GDS propagates back up the beam line until it reflects off the input

surface of the THG, passes back though the GDS and eventually comes to a focus on a pane of Borofloat® glass. Inspection of the armor glass found a section of damage where the ghost is calculated to focus. The addition of an anti-reflection coating on the exit surface of the GDS reduced the intensity of the ghost generating the SuperGrey™ particles sufficiently to effectively eliminate particle production. Figure 12 shows a schematic of the two sources of particles and the mitigations which eliminated them from the GDS.

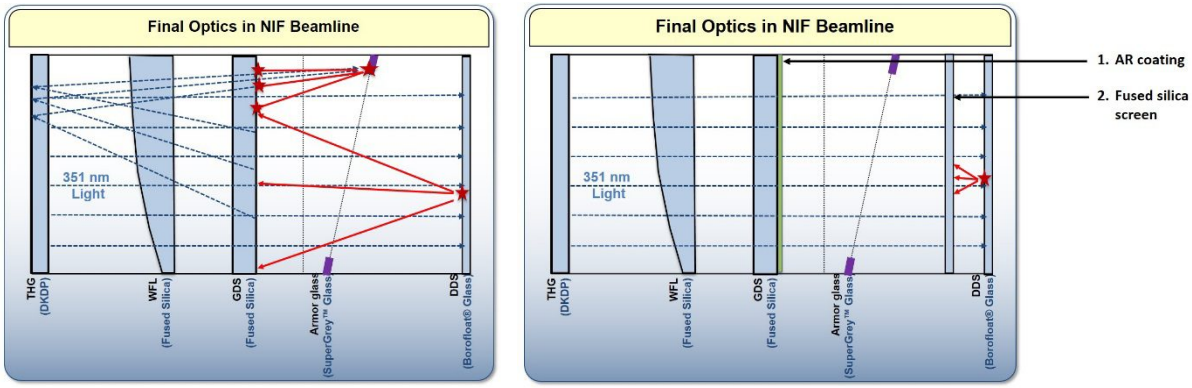

Figure 12. Left: Two particle sources were identified as responsible for damage on the GDS. Right: Particle deposition on the GDS was eliminated by the addition of a Fused silica screen and an AR coating.

In addition to the engineered solutions discussed above, we have also studied procedural solutions in which the sequence of laser shots can be altered to reduce the total damage incurred by the GDS optics. We have cataloged the amount and size of particles produced by both SuperGrey™ as well as Borofloat® as a function of laser fluence (figure 13). The probability of particles damaging as a function of size for each material type was documented for both coated and uncoated SiO_2 substrates (figure 14). We found that the coating may provide some small amount of protection against damage induced by SuperGrey particles but not ejecta from ISBEs.

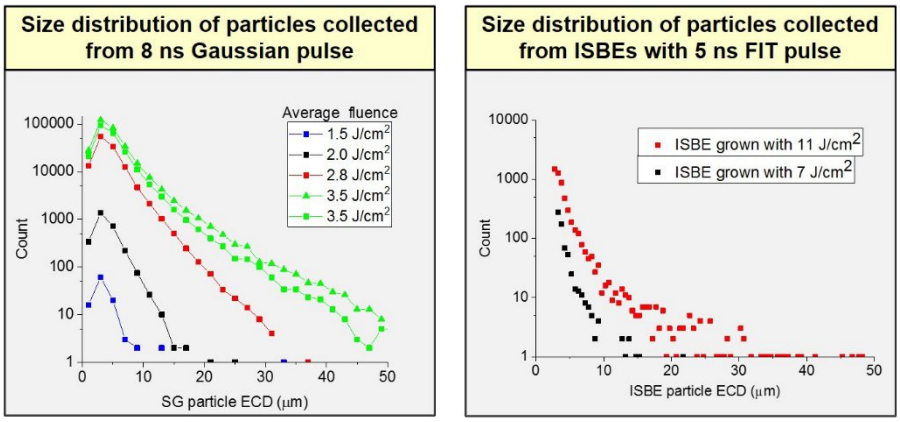

Figure 13. Left: A family of particle size histograms produced by exposing SuperGray™ to 8 ns 3ω pulses of various fluences. Right: Size histograms of particle sizes produced by exposing an already erupted ISBE to 7-J/cm^2 and 11-J/cm^2 3ω 5-ns pulses.

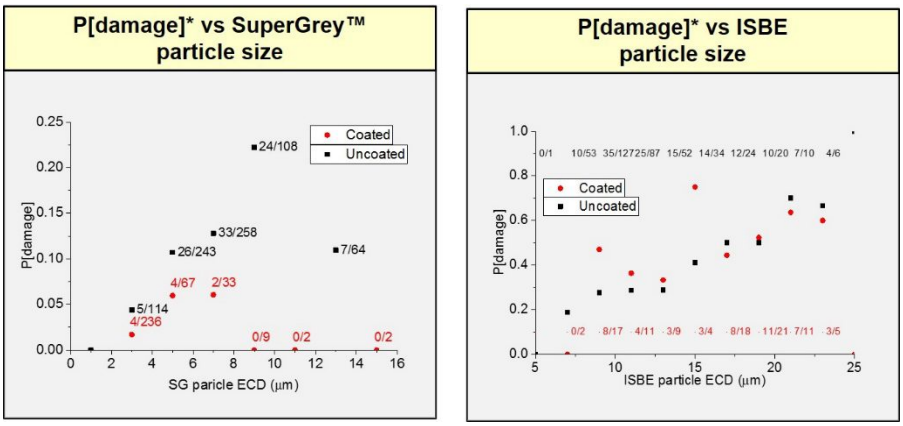

Figure 14. Left: Probability of SuperGrey™ particles producing damage as a function of size when exposed to 9.5-J/cm^2 3ω 5-ns pulses. Right: Probability of ISBE ejecta to produce damage on coated and uncoated SiO_2 substrates when exposed to 9 J/cm^2.

We have also found that pre-exposure of both particle types to pulses of lower fluence can clean the particles without producing growing damage and reduce the total damage when subsequently exposed to 9 J/cm^2 pulses. The reduction in damage is dependent on the fluence, number of exposures and pulse duration of the cleaning pulses. Fluences below around 3.5 J/cm^2 produced no laser cleaning and fluences above around 7 J/cm^2 caused more particles to damage than to clean. The optimal cleaning fluence for both SuperGrey™ particles as well as ISBE ejecta was around 6 J/cm^2 for the 3ω 5-ns FIT pulses used here. Based on other initiation and growth studies, one would expect that the cleaning effect would be pulse length (and perhaps shape) dependent as well[23].

3. MANAGING PARTICLE INDUCED DAMAGE

A second experiment on NIF tested mixtures of the three mitigations (laser cleaning, AR coated GDS, and fused silica debris shields (FSDS)) to exposure to ten 1.8 MJ equivalent shots (about 9.5 J/cm^2 of 3ω in this case). We found that beam lines with AR coatings on the GDS had an average number of damage sites a factor of 5 lower than the average for the control beams. Beam cleaning reduced the number of growing sites by an additional factor of 10. The combination of AR coatings on the GDS and FSDS reduced growing damage sites by a factor of 200 and total damage by three orders of magnitude (see figure 15) as compared to the control beams.

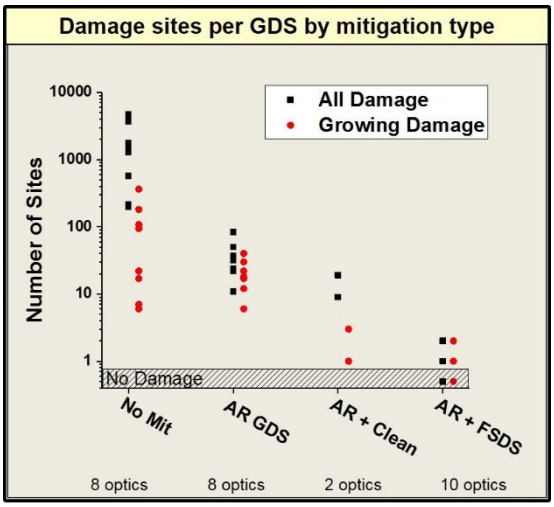

Figure 15. Total number damage sites and number of growing damage sites on NIF GDSs optics installed for several combinations of the developed mitigations. No Mit beams had no mitigations and were the control beams for the experiment. The number of optics listed below each cluster of data is the number that participated in that experiment type.

4. CONCLUSION

In conclusion, since the implementation of the AMP process for NIF's SiO_2 optics, the vast majority of damage has been due to particle contamination. Here we show that two types of particle sources were especially prevalent, namely material ejected from bulk damage in the DDS which has grown sufficiently to breach its input surface and particles generated by a ghost focusing on absorbing glass. Moreover that debris in itself is largely benign and only initiates damage if it arrives on the surface of the receiving optic with high temperatures and velocities.

Damage on the GDS can be reduced by three orders of magnitude by the implementation of two engineered solutions, namely an AR coating applied to the exit surface of the GDS itself and a SiO_2 screen installed between the GDS and the DDS. Altering the order of laser pulses to enhance laser cleaning was demonstrated to have a 10x reduction in damage alone.

5. ACKNOWLEDGEMENTS

This work was performed under the auspices of the U.S. Department of Energy by Lawrence Livermore National Laboratory under contract DE-AC52-07NA27344. Lawrence Livermore National Security, LLC

6. REFERENCES

1. Spaeth, M.L., et al., *Description of the NIF Laser.* Fusion Science and Technology, 2016. **69**(1): p. 25-145.
2. Fleurot, N., C. Cavailler, and J.L. Bourgade, *The Laser Megajoule (LMJ) Project dedicated to inertial confinement fusion: Development and construction status.* Fusion Engineering and Design, 2005. **74**(1-4): p. 147-154.
3. Spaeth, M.L., et al., *Optics Recycle Loop Strategy for NIF Operations Above UV Laser-Induced Damage Threshold.* Fusion Science and Technology, 2016. **69**(1): p. 265-294.
4. Carr, C.W., et al., *The effect of laser pulse shape and duration on the size at which damage sites initiate and the implications to subsequent repair.* Optics Express, 2011. **19**(14): p. A859-A864.
5. Bass, I.L., et al., *Mitigation of laser damage growth in fused silica NIF optics with a galvanometer scanned CO2 laser.* High-Power Laser Ablation Vi, Pts 1 and 2, 2006. **6261**.

6. Bass, I.L., et al., *An Improved Method of Mitigating Laser Induced Surface Damage Growth in Fused Silica Using a Rastered, Pulsed CO2 Laser.* Laser-Induced Damage in Optical Materials: 2010, 2010. **7842**.
7. Negres, R.A., et al., *Growth model for laser-induced damage on the exit surface of fused silica under UV, ns laser irradiation.* Optics Express, 2014. **22**(4): p. 3824-3844.
8. Honig, J., et al., *Experimental study of 351-nm and 527-nm laser-initiated surface damage on fused silica surfaces due to typical contaminants.* Laser-Induced Damage in Optical Materials: 2004, 2005. **5647**: p. 129-135.
9. Negres, R.A., et al., *Exploration of the multiparameter space of nanosecond-laser damage growth in fused silica optics.* Applied Optics, 2011. **50**(22): p. D12-D20.
10. Norton, M.A., et al., *Growth of laser damage on the input surface of SiO2 at 351 nm.* Laser-Induced Damage in Optical Materials: 2006, 2007. **6403**.
11. Gallais, L. and J.Y. Natoli, *Optimized metrology for laser-damage measurement: application to multiparameter study.* Applied Optics, 2003. **42**(6): p. 960-971.
12. Suratwala, T.I., et al., *HF-Based Etching Processes for Improving Laser Damage Resistance of Fused Silica Optical Surfaces.* Journal of the American Ceramic Society, 2011. **94**(2): p. 416-428.
13. Bude, J., et al., *Silica laser damage mechanisms, precursors and their mitigation.* Laser-Induced Damage in Optical Materials: 2014, 2014. **9237**.
14. Negres, R.A., et al., *Probability of growth of small damage sites on the exit surface of fused silica optics.* Optics Express, 2012. **20**(12): p. 13030-13039.
15. Shen, N., J.D. Bude, and C.W. Carr, *Model laser damage precursors for high quality optical materials.* Optics Express, 2014. **22**(3): p. 3393-3404.
16. Demos, S.G., et al., *Morphology of ejected debris from laser super-heated fused silica following exit surface laser-induced damage.* Laser-Induced Damage in Optical Materials: 2015, 2015. **9632**.
17. Raman, R.N., et al., *Damage on fused silica optics caused by laser ablation of surface-bound microparticles.* Optics Express, 2016. **24**(3): p. 2634-2647.
18. Carr, C.W., et al., *The effect of laser pulse duration on laser-induced damage in KDP and SiO2.* Laser-Induced Damage in Optical Materials: 2006, 2007. **6403**.
19. Schott. *Borofloat® glass*. 2017; Available from: http://www.us.schott.com/borofloat/english/index.html.
20. Matthews, M.J., et al., *Laser-matter coupling mechanisms governing particulate induced damage on optical surfaces.* Laser-Induced Damage in Optical Materials 2016, 2016. **10014**.
21. Bude, J., et al., *Particle damage sources for fused silica optics and their mitigation on high energy laser systems.* Optics Express, 2017. **25**(10): p. 11414-11435.
22. Pilkington. *SuperGreyTM*. 2017; Available from: http://www.pilkington.com/north-america/usa/english/products/bp/byben.
23. Carr, C.W., J.B. Trenholme, and M.L. Spaeth, *Effect of temporal pulse shape on optical damage.* Applied Physics Letters, 2007. **90**(4).